

Universal Short Range Correlations in Bosonic Helium Clusters

B. Bazak,¹ M. Valiente,² and N. Barnea¹

¹The Racah Institute of Physics, The Hebrew University, 9190401, Jerusalem, Israel

²Institute for Advanced Study, Tsinghua University, Beijing 100084, China

(Dated: January 24, 2020)

Short-range correlations in bosonic Helium clusters, composed of ${}^4\text{He}$ atoms, are studied utilizing the generalized contact formalism. The emergence of universal n -body short range correlations is formulated and demonstrated numerically via Monte Carlo simulations. The values of the n -particle contacts are evaluated for $n \leq 5$. In the thermodynamic limit, the two-body contact is extracted from available experimental measurements of the static structure factor of liquid ${}^4\text{He}$ at high momenta, and found in a good agreement with the value extracted from our calculations.

Interacting multiparticle systems where the interaction range is much smaller than any other characteristic length scale, such this associated with the density or the average momentum, can be studied using the zero range approximation. In this limit, the interaction details are neglected and the system acquires universal features depending only on its density ρ and the scattering length a_s . When a_s is small, the particles interact weakly and the system is amenable to perturbative treatment. When it is large, the particles are strongly correlated and one needs to resort to numerical methods to study the system properties.

About a decade ago, while studying two-component Fermi systems with large a_s , Tan has succeeded to show that many of its properties are governed by a single parameter, the so-called *contact* C , which measures the probability of two particles being in close proximity [1]. Following Tan's work, different relations between various properties of such system and the contact, known as the *Tan relations*, were derived and verified experimentally with ultracold gases [2–5]. One example is the one-body momentum distribution $n(k)$ tail, determined to be

$$\lim_{k \rightarrow \infty} n(k) = C/k^4. \quad (1)$$

The Pauli principle prevents identical fermions from approaching each other in a relative s -wave state. Consequently, three-body correlations are typically negligible in an ultracold two-component atomic Fermi gas. In contrast, such three-body coalescence is expected to play a decisive role in bosonic gases or for nucleons, where the spin- $\frac{1}{2}$ neutrons and protons form a four-component Fermi system. Indeed for bosonic systems, the tail of the momentum distribution is predicted to include a sub-leading k^{-5} term, emerging from such three-body correlations [6]. We note that other singular interactions, like Coulomb, also exhibit universal short-distance correlations [7, 8].

To derive the *Tan relations* one may start with the observation that when two particles approach each other, the N -body wavefunction is factorized into a product of a universal 2-body function ϕ_2 and a state-dependent function $A_N^{(2)}$ describing the residual system,

$$\Psi(\mathbf{r}_1, \dots, \mathbf{r}_N) \xrightarrow{r_{ij} \rightarrow 0} \phi_2(\mathbf{r}_{ij}) A_2^{(N)}(\mathbf{R}_{ij}, \{\mathbf{r}_k\}_{k \neq i,j}). \quad (2)$$

Here $\mathbf{r}_{ij} = \mathbf{r}_i - \mathbf{r}_j$ is the interparticle distance and $\mathbf{R}_{ij} = (\mathbf{r}_i + \mathbf{r}_j)/2$ is the pair's center of mass coordinate. In the zero-range approximation the universal pair wavefunction is given by $\phi_2(\mathbf{r}_{ij}) = 1/r_{ij} - 1/a_s + O(r_{ij})$.

Recently, the contact formalism was generalized to systems where the zero-range approximation is not justified [9–13]. This is the situation, for example, in the atomic nucleus, where the interparticle distance is about 2.4 fm, while the nuclear interaction range, estimated from the pion mass, is about $\hbar/m_\pi c \approx 1.4$ fm. This is also the situation in ${}^4\text{He}$ atomic clusters, where the average interparticle distance within clusters with more than three atoms is about 5 Å, while the van der Waals length, characterizing the potential's range, is about 5.4 Å.

In such cases, one would not expect to see a *strong* universality, i.e. relations which do not depend on the interaction details and are determined only by scattering parameters such as a_s . Still, given an interaction model strong at small distances, the wavefunction factorization (Eq. 2) remains valid since at close distance a correlated particle pair is barely influenced by the surrounding particles and therefore its wavefunction $\phi_2(\mathbf{r})$ should be the same regardless of the system size or state. We will call this situation *weak* universality.

It is instructive therefore to study the adaptation of Tan's relations to weak universality. For instance, relations between the one and two-body momentum distributions as well as the two-body density were studied in nuclei [10, 11]. In the following we will investigate such relations for bosonic ${}^4\text{He}$ clusters.

${}^4\text{He}$ clusters have attracted a lot of attention. For a long time, the ${}^4\text{He}$ trimer seemed to be the most promising candidate for experimental validation of the Efimov effect [14], as liquid Helium was for Bose-Einstein condensation. Recently ${}^4\text{He}$ dimer and trimer densities were measured experimentally [15, 16]. The results compare very well with theoretical calculations using ${}^4\text{He}$ pair potential models. The dimer and trimer densities at short range play a crucial role in the contact formalism we study here. The atomic clusters exhibit a universal short-range 2, 3-body behavior stemming from the dimer and trimer wavefunctions, respectively. Moreover, this phenomenon also continues with the coalescence of more atoms inside these clusters, showing the emergence of

4, 5, ...-body universality.

In order to study the properties of ^4He clusters we solve the N -body Schrödinger equation with the LM2M2 pair potential [17].

As we argued above, in the limit of vanishing interparticle distance $r \rightarrow 0$ we expect the wavefunction Ψ to factorize as in Eq. (2) into a universal 2-body function and a residual state dependent function. If true, this factorization holds also for $N = 2$. Consequently, we can identify ϕ_2 with the dimer wavefunction.

The resulting two-body contact is defined as the norm of the residual non-universal part of the wavefunction multiplied by the number of pairs,

$$C_2^{(N)} = \frac{N(N-1)}{2} \langle A_2^{(N)} | A_2^{(N)} \rangle = \binom{N}{2} \langle A_2^{(N)} | A_2^{(N)} \rangle. \quad (3)$$

Using this definition, the pair density function at short distances attains an extremely simple form,

$$\rho_2^{(N)}(r) = \langle \Psi | \hat{\rho}_2^{(N)}(r) | \Psi \rangle \xrightarrow{r \rightarrow 0} C_2^{(N)} \rho_2(r) \quad (4)$$

where $\hat{\rho}_2^{(N)}(r) = \frac{1}{r^2} \sum_{i < j} \delta(r_{ij} - r)$, $\rho_2(r) \equiv \rho_2^{(2)}(r) = \int d\Omega_2 |\phi_2(\mathbf{r})|^2$, and Ω_2 is the solid angle.

In a bosonic system, coalescence of more particles should provide further factorizations of the wavefunction [18]. When particles i, j and k come close together, the wavefunction is factorized as

$$\Psi \xrightarrow{r_{ijk} \rightarrow 0} \phi_3(\mathbf{x}_{ijk}, \mathbf{y}_{ijk}) A_3^{(N)}(\mathbf{R}_{ijk}, \{\mathbf{r}_l\}_{l \neq i, j, k}) \quad (5)$$

where the triplet wavefunction depends on the Jacobi coordinates $\mathbf{x}_{ijk} = \sqrt{1/2}(\mathbf{r}_i - \mathbf{r}_j)$ and $\mathbf{y}_{ijk} = \sqrt{2/3}(\mathbf{r}_k - (\mathbf{r}_i + \mathbf{r}_j)/2)$, and the factorization holds for small hyper-radius $r_{ijk}^2 = x_{ijk}^2 + y_{ijk}^2$. Here \mathbf{R}_{ijk} is the three body center of mass coordinate. In analogy with Eq. (3), the three-body contact in the N -body system is defined to be the number of triplets times the norm of the particular part of the wavefunction in three-body coalescence,

$$C_3^{(N)} = \binom{N}{3} \langle A_3^{(N)} | A_3^{(N)} \rangle. \quad (6)$$

The triplet density operator is defined as,

$$\hat{\rho}_3^{(N)}(r) = \frac{1}{r^5} \sum_{i < j < k} \delta(r_{ijk} - r) \quad (7)$$

and its expectation value in the N -body system is

$$\rho_3^{(N)}(r) = \langle \psi | \hat{\rho}_3^{(N)}(r) | \psi \rangle \xrightarrow{r \rightarrow 0} C_3^{(N)} \rho_3(r) \quad (8)$$

where $\rho_3(r) \equiv \rho_3^{(3)}(r) = \int d\Omega_3 |\phi_3(\mathbf{x}, \mathbf{y})|^2$, and Ω_3 denotes the hyperangles associated with \mathbf{x} , and \mathbf{y} .

Similar factorization is assumed in the n -body coalescence, leading to the definition of the n -body contact, and to the n -body density function,

$$\rho_n^{(N)}(r) \xrightarrow{r \rightarrow 0} C_n^{(N)} \rho_n(r), \quad (9)$$

where here $r = \sqrt{\sum_{i < j}^n (\mathbf{r}_i - \mathbf{r}_j)^2 / n}$ is the n -body hyperradius. This is one of the main results of this paper and in the following we shall show that this is indeed the case for $n \leq 5$ in atomic ^4He droplets with N atoms. In the mean time we note that with the above definition the contact for $n = N$ equals unity since $\rho_n(r) \equiv \rho_n^{(n)}(r)$.

Using this factorization, the zero-range result for the high momentum limit of the 1-body momentum distribution (Eq. 1), is now modified to get [19]

$$n^{(N)}(\mathbf{k}) \xrightarrow{k \rightarrow \infty} 2C_2^{(N)} |\tilde{\phi}_2(\mathbf{k})|^2 \quad (10)$$

where $\tilde{\phi}_2(\mathbf{k})$ is the Fourier transform (FT) of $\phi_2(\mathbf{r})$. The high momentum limit of the static structure factor, which is proportional to the contact in the zero-range limit [5], gets now the form

$$S(Q) \xrightarrow{Q \rightarrow \infty} 1 + \frac{2C_2^{(N)}}{N} \frac{4\pi}{Q} \int dr r \sin(Qr) \rho_2(r), \quad (11)$$

where Q is the momentum transfer. It is also possible to relate the contact to the potential energy which, for a cluster of bosons interacting via 2-body forces can be written using the 2-body density $\langle V_2^{(N)} \rangle = \int d\mathbf{r} \rho_2^{(N)}(r) v(r)$. For a short range interaction we can replace $\rho_2^{(N)}$ by its asymptotic form, Eq. (4), relating the N -body potential energy to the 2-body contact and potential energy [19],

$$\langle V_2^{(N)} \rangle = C_2^{(N)} \langle V_2^{(2)} \rangle, \quad (12)$$

which generalizes the zero-range result of Ref. [20].

The N dependence - To understand the dependence of the n -body contact on the total particle number N in the cluster, it is useful to relate the pair density $\rho_2^{(N)}$ to the 2-body density $\chi(\mathbf{r}, \mathbf{r}') = \sum_{i \neq j} \langle \Psi | \delta(\mathbf{r} - \mathbf{r}_i) \delta(\mathbf{r}' - \mathbf{r}_j) | \Psi \rangle$, namely

$$\rho_2^{(N)}(\mathbf{r}_{12}) = \frac{1}{2} \int d\mathbf{R}_{12} \chi(\mathbf{r}_1, \mathbf{r}_2). \quad (13)$$

In the limit $N \rightarrow \infty$ the system becomes homogeneous, $\chi(\mathbf{r}_1, \mathbf{r}_2) \rightarrow \chi(\mathbf{r}_{12})$ and therefore $\rho_2^{(N)}(\mathbf{r}_{12}) = V\chi(\mathbf{r}_{12})/2 = N\chi(\mathbf{r}_{12})/2\rho$ where V is the volume of the system and $\rho = N/V$ is the density. Taking now the limit $r_{12} \rightarrow 0$ one can get the relation [19]

$$\chi(r) \xrightarrow{r \rightarrow 0} 2\rho \frac{C_2^{(N)}}{N} \rho_2(r). \quad (14)$$

We know that in the thermodynamic limit χ and ρ are finite. It follows that $C_2^{(N)} \propto N$ as $N \rightarrow \infty$. The same argument can be repeated for $n = 3, 4, 5, \dots$ leading to the general conclusion that for any n -body coalescence $C_n^{(N)} \propto N$ as $N \rightarrow \infty$. Equipped with this observation it seems natural to define a reduced contact $\tilde{C}_n^{(N)} \equiv C_n^{(N)}/N$. As the atomic He clusters behave very

much like a cluster of rigid balls, we expect that the leading corrections to the above argument will depend on the ratio between surface particles $\propto N^{2/3}$ and volume particles $\propto N$. Consequently in the limit $N \rightarrow \infty$ the contacts are expected to have the following N dependence

$$\tilde{C}_n^{(N)} = \tilde{C}_n^\infty + \alpha_n N^{-1/3} + \beta_n N^{-2/3} + \dots \quad (15)$$

The computational method - Throughout the years, a variety of numerical methods have been developed to solve the few-body Schrödinger equation. However, the increasing dimensionality and the hard-core nature of the ${}^4\text{He}$ - ${}^4\text{He}$ pair potential make this problem hard to handle for most numerical methods. Here we use the Variational Monte Carlo (VMC) and Diffusion Monte Carlo (DMC) methods. Since these methods are well-known we will only describe them very briefly, for a comprehensive review see e.g. [21].

Given a trial wave-function Ψ_T , the variational energy

$$E_{var} = \frac{\langle \Psi_T | H | \Psi_T \rangle}{\langle \Psi_T | \Psi_T \rangle} \geq E_0 \quad (16)$$

is an upper bound to the true ground-state energy E_0 . In the VMC method the integrals in Eq. (16) are evaluated using the Monte Carlo numerical integration technique, typically the Metropolis algorithm [22]. Using the variational principle (16), parameters characterizing Ψ_T can be optimized, minimizing the trial energy or its variance.

DMC is an alternative approach to solve the Schrödinger equation through propagation of the solution in imaginary time $\tau = -it$,

$$\frac{\partial \Psi(\mathbf{r}_1 \dots \mathbf{r}_N, \tau)}{\partial \tau} = (T + V - E_R) \Psi(\mathbf{r}_1 \dots \mathbf{r}_N, \tau). \quad (17)$$

where E_R is a reference energy. Eq. (17) is treated as a diffusion-reaction process for so-called walkers, distributed according to Ψ . As time propagates, Ψ will be dominated by the eigenstate with the lowest energy which has a non-zero overlap with the initial state. All other eigenstates will decay exponentially faster. The ground state energy is the reference energy which conserves the walkers number.

Improved results are obtained by introducing a trial wavefunction to guide the diffusion process, therefore a typical DMC calculation starts with an optimized VMC wave-function. We adopt the trial wavefunction form of Ref. [23], $\Psi_T = \prod_{i < j} f(r_{ij})$ where

$$f(r) = \exp[-(p_5/r)^5 - (p_2/r)^2 - p_1 r] / r^{p_0}. \quad (18)$$

Here p_5, p_2, p_1 , and p_0 are variational parameters, which can be found in Ref. [24].

Ground state energies - To benchmark our Monte Carlo code we have calculated the ground-state energies of small ${}^4\text{He}$ clusters with the LM2M2 pair-potential. Calculations were done with 4000 walkers, using 10000 blocks of 500 iterations each. The first 100 blocks were used for equilibration.

Table I: The ground-state energies (in mK) of small ${}^4\text{He}$ clusters, with the LM2M2 pair-potential. The dimer energy is 1.30348 mK [32].

N	Ref [31]	Ref [32]	Ref [29]	Ref [30]	This work
3	126.39	126.40	125.5(6)	124(2)	125.9(2)
4	557.7	558.98	557(1)	558(3)	557.4(4)
5			1296(1)	1310(5)	1300(2)
6			2309(3)	2308(5)	2315(2)
7			3565(4)	3552(6)	3571(2)
8			5020(4)	5030(8)	5041(2)
9			6677(6)	6679(9)	6697(2)
10			8495(7)	8532(10)	8519(3)

The ${}^4\text{He}$ trimer ground state energy using this potential has been calculated using several few-body techniques. Most results agree with $B_3 = 126.0(5)$ mK [25–32], while different values also exist [33, 34].

Few calculations have been done for larger clusters. The tetramer energy was calculated in Refs. [29–32] using the LM2M2 potential. In Ref. [35] a soft-core potential was used while in Refs. [36, 37] an effective field theory approach was followed. In both cases the interaction parameters were fitted to the LM2M2 potential. Larger clusters were investigated using the DMC method [29, 30]. In Table I we compare these calculations with our results, showing good agreement with the published binding energies.

The n -body density function - To calculate the n -body densities we have used a combination of VMC and DMC estimates,

$$\langle \hat{O} \rangle = 2\langle \hat{O} \rangle_{\text{DMC}} - \langle \hat{O} \rangle_{\text{VMC}} \quad (19)$$

where $\langle \hat{O} \rangle_{\text{DMC}} = \langle \Psi_T | \hat{O} | \Psi \rangle / \langle \Psi_T | \Psi \rangle$ is the mixed DMC estimate, and $\langle \hat{O} \rangle_{\text{VMC}} = \langle \Psi_T | \hat{O} | \Psi_T \rangle / \langle \Psi_T | \Psi_T \rangle$ is the VMC estimate. This result is accurate to second order in the wavefunction $O(\delta\Psi^2)$, $\delta\Psi = \Psi_T - \Psi$ [38]. Moreover, we checked our results with pure-estimator based on the descendant weighting method [39], and found no significant change.

For the smaller clusters, the resulting n -body densities exhibit a typical bell shape, starting from zero at $r = 0$, reaching a maximum value, and finally falling exponentially at large r . According to Eq. (4), we expect that at short distances the pair density function $\rho_2^{(N)}$ will coincide with the dimer density ρ_2 up to a scaling factor, the 2-body contact $C_2^{(N)}$, which we can extract fitting these two functions [40]. This situation is expected to repeat itself for the 3-body density function, Eq. (8), and in general for any n -body density, Eq. (9).

Having extracted the contacts [40] we are in position to demonstrate the validity of Eq. (9). To this end, we plot in Fig. 1 the normalized n -body densities $\rho_n^{(N)} / C_n^{(N)}$

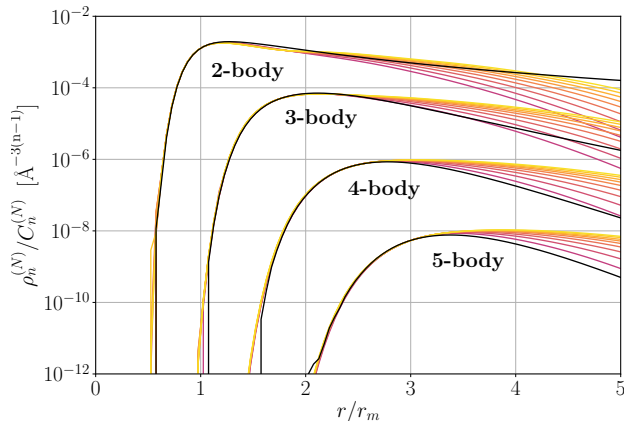


Figure 1: The n -body density function normalized with the appropriate contact $\rho_n^{(N)}/C_n^{(N)}$ is presented as function of the n -body radius for $n = 2, 3, 4, 5$. For each n the reference density ρ_n is drawn with a black line. The densities for $N = 10, 15, 20 \dots 50$, are given by the colored lines (from dark to light).

Table II: The asymptotic values of the reduced n -body contacts $\tilde{C}_n^{(N)} = C_n^{(N)}/N$ of ${}^4\text{He}$ droplets.

n	2	3	4	5
\tilde{C}_n^∞	230 ± 25	500 ± 60	1800 ± 300	5900 ± 1000

as a function of the n -body radius r/r_m . $r_m = 2.6965\text{\AA}$ being the minimum 2-body potential locus. The plot contains results for ${}^4\text{He}$ clusters with $N = n$ and $N = 10, 15, 20, \dots 50$ particles. Inspecting the plot we see that, indeed, for each n there is a range r_n such that for $r \leq r_n$ all the normalized densities collapse into a single curve. For the pair density this range is approximately $1.3r_m$ and it grows linearly with n , i.e. $r_n \approx n 0.65r_m$.

The numerical values of the extracted contacts are presented in the supplementary material [24]. Here we analyze the N dependence of the n -body contacts. From Eq. (15) we expect $\tilde{C}_n^{(N)} = C_n^{(N)}/N$ to be finite in the thermodynamic limit. Our MC code was designed to study small He clusters with $N \leq 50$ particles, and is therefore ill-equipped to study this $N \rightarrow \infty$ limit. Instead, to estimate \tilde{C}_n^∞ we fit our calculated contacts to Eq. (15). Doing so, we have found that, for $N \geq 10$, 3 terms are enough to describe $C_2^{(N)}$, $C_3^{(N)}$, and 4 terms for $C_4^{(N)}$, $C_5^{(N)}$. The asymptotic values of the reduced contacts are given in Table II. The calculated contacts are plotted together with the asymptotic expansion in Fig. 2, where we observe that the calculated values are well reproduced by the asymptotic expansion.

Having calculated the 2-body contacts, the $Q \rightarrow \infty$ limit of the structure factor can be evaluated for any

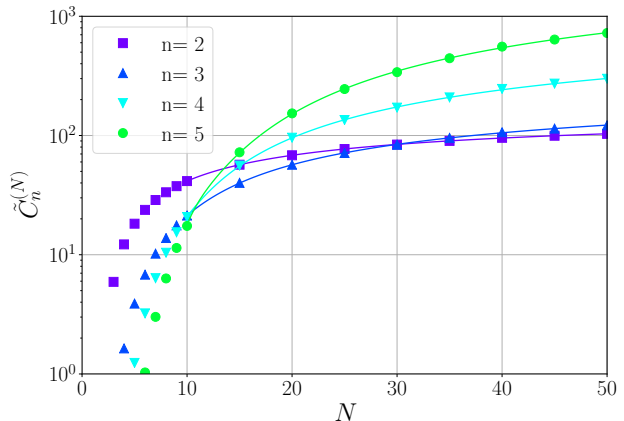


Figure 2: The evolution of the reduced n -body contacts $\tilde{C}_n^{(N)} = C_n^{(N)}/N$ with the system size N . Symbols - calculated values, curves - the asymptotic expansion given in Eq. (15).

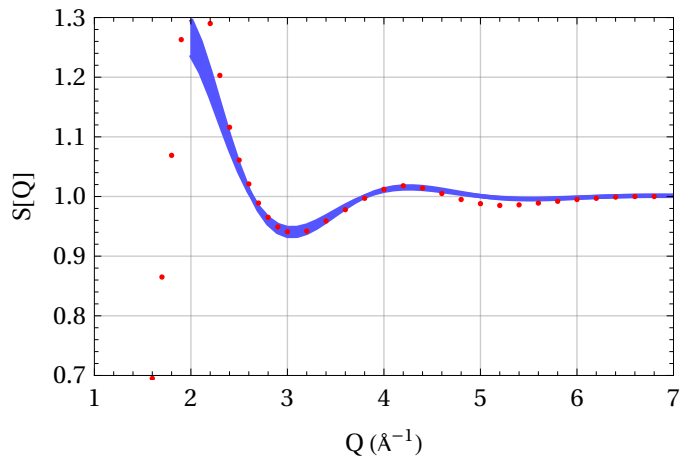


Figure 3: The structure factor of liquid ${}^4\text{He}$ as a function of the momentum transfer Q , a comparison between the experimental data of Svensson *et al.* [43] and the contact theory, Eq. (11). The experimental data are presented by dots. The band corresponds to calculated contact values in the range $\tilde{C}_2^\infty \in (200, 250)$.

helium droplet and compared with experiment.

For liquid helium, the structure factor was measured using x-ray scattering [41, 42], and neutron scattering techniques [43]. Following the analysis of Donnelly and Barenghi [44] we adopt the latter data set and compare it with the contact theory, Fig. 3. In the range $Q \geq 2\text{\AA}^{-1}$, dominated by the short-range pair function ϕ_2 , we see a nice agreement between the two. The data fits contact values in the range $\tilde{C}_2^\infty \in (200, 250)$ as predicted by our calculations, Tab. II.

The dynamic structure factor $S(Q, E)$ of liquid ${}^4\text{He}$ was recently measured by Prisk *et al.* [45], using the

neutron Compton scattering technique. In the impulse approximation, $S(Q, E)$ and consequently the neutron Compton profile can be calculated from the 1-body momentum distribution $n(\mathbf{k})$. Utilizing the contact relation (10), we analyzed these results. Overall we got reasonable agreement between the data and the theory for contact values $\tilde{C}_2^\infty = 180 \pm 40$, a value consistent with both the MC calculation and the static structure factor data.

Conclusion. Summing up, utilizing the generalized contact formalism, we have studied short-range correlations in bosonic Helium clusters composed of ^4He atoms. Specifically, we have studied n -body coalescences, and the emergence of universal n -body short-range correlations. Employing the LM2M2 pair potential, VMC and DMC calculations were used to demonstrate and verify the universal nature of these correlations. For systems with up to $N = 50$ particles, the values of the n -body contacts were evaluated numerically for $n \leq 5$. The thermodynamic limit was studied, extrapolating our numerical results. Comparing our prediction with the experi-

mental two-body contact, extracted from available measurements of the structure factor of liquid ^4He at high momenta, we have found a good agreement. It would be interesting to compare our predictions with detailed Monte Carlo simulations of Helium liquid.

The implications of the current formalism on the momentum distribution and the dynamic structure factors call for further experimental studies in the high momentum sector.

Acknowledgments

We would like to thank Reinhard Dörner, Gregory Astrakharchik, Dmitry Petrov, Lorenzo Contessi and Ronen Weiss for useful discussions and communications. We thank Timothy R. Prisk for sharing the experimental data of Ref. [45] with us. The work of N.B was supported by the Pazy foundation.

-
- [1] S. Tan, Energetics of a strongly correlated Fermi gas, *Ann. Phys. (N.Y.)* **323**, 2952 (2008); Large momentum part of a strongly correlated Fermi gas, *Ann. Phys. (N.Y.)* **323**, 2971 (2008); Generalized virial theorem and pressure relation for a strongly correlated Fermi gas, *Ann. Phys. (N.Y.)* **323**, 2987 (2008).
- [2] J. T. Stewart, J. P. Gaebler, T. E. Drake, and D. S. Jin, Verification of Universal Relations in a Strongly Interacting Fermi Gas, *Phys. Rev. Lett.* **104**, 235301 (2010).
- [3] Y. Sagi, T. E. Drake, R. Paudel, and D. S. Jin, Measurement of the Homogeneous Contact of a Unitary Fermi Gas, *Phys. Rev. Lett.* **109**, 220402 (2012).
- [4] F. Werner, L. Tarruel, and Y. Castin, Number of closed-channel molecules in the BEC-BCS crossover, *Eur. Phys. J. B* **68**, 401 (2009).
- [5] E. D. Kuhnle, H. Hu, X.-J. Liu, P. Dyke, M. Mark, P. D. Drummond, P. Hannaford, and C. J. Vale, Universal Behavior of Pair Correlations in a Strongly Interacting Fermi Gas, *Phys. Rev. Lett.* **105**, 070402 (2010).
- [6] E. Braaten, D. Kang, and L. Platter, Universal Relations for Identical Bosons from Three-Body Physics, *Phys. Rev. Lett.* **106**, 153005 (2011).
- [7] J. C. Kimball, Short-Range Correlations and Electron-Gas Response Functions, *Phys. Rev. A* **7**, 1648 (1973).
- [8] J. Hofmann, M. Barth, and W. Zwerger, Short-distance properties of Coulomb systems, *Phys. Rev. B* **87**, 235125 (2013).
- [9] R. Weiss, B. Bazak, and N. Barnea, Nuclear Neutron-Proton Contact and the Photoabsorption Cross Section, *Phys. Rev. Lett.* **114**, 012501 (2015).
- [10] R. Weiss, B. Bazak, and N. Barnea, Generalized nuclear contacts and momentum distributions, *Phys. Rev. C* **92**, 054311 (2015).
- [11] R. Weiss, R. Cruz-Torres, N. Barnea, E. Piasetzky, and O. Hen, The nuclear contacts and short range correlations in nuclei, *Phys. Lett. B* **780**, 211 (2018).
- [12] G. A. Miller, Non-universal and universal aspects of the large scattering length limit, *Phys. Lett. B* **777**, 442 (2018).
- [13] F. Werner and Y. Castin, General relations for quantum gases in two and three dimensions: Two-component fermions, *Phys. Rev. A* **86**, 013626 (2012).
- [14] V. Efimov, Energy levels arising from resonant two-body forces in a three-body system, *Phys. Lett. B* **33**, 563 (1970).
- [15] S. Zeller *et al.*, Imaging the He_2 quantum halo state using a free electron laser, *Proc. Natl. Acad. Sci. U.S.A.* **113**, 14651 (2016).
- [16] J. Voigtsberger *et al.*, Imaging the structure of the trimer systems $^4\text{He}_3$ and $^3\text{He}^4\text{He}_2$, *Nat. C.* **5**, 5765 (2014).
- [17] R. A. Aziz and M. J. Slaman, An examination of ab initio results for the helium potential energy curve, *J. Chem. Phys.* **94**, 8047 (1991).
- [18] F. Werner and Y. Castin, General relations for quantum gases in two and three dimensions. II. Bosons and mixtures, *Phys. Rev. A* **86**, 053633 (2012).
- [19] Eqs. (10), (12), and (14) were derived by Werner and Castin in [13]. However, their definition of the 2-body contact $C = 4\pi m/\hbar^2 dE/d(-1/a_s)$ differs from ours. The two definitions coincide in the zero-range limit.
- [20] S. Zhang and A. J. Leggett, Universal properties of the ultracold Fermi gas *Phys. Rev. A* **79**, 023601 (2009)
- [21] M. H. Kalos and P. A. Whitlock, *Monte Carlo Methods*, (WILEY-VCH, Weinheim, 2008.)
- [22] N. Metropolis, A. W. Rosenbluth, M. N. Rosenbluth, A. H. Teller, and E. Teller, Equations of state calculations by fast computing machines, *J. Chem. Phys.* **21**, 1087 (1953).
- [23] S. W. Rick, D. L. Lynch, and J. D. Doll, A variational Monte Carlo study of argon, neon, and helium clusters, *J. Chem. Phys.* **95**, 3506 (1991).
- [24] See Supplemental Material at XXX for the numerical values of the trial wave function parameters and for the extracted contact values.
- [25] E. Nielsen, D. V. Fedorov, and A. S. Jensen, The structure of the atomic helium trimers: halos and Efimov

- states, *J Phys B* **31**, 4085 (1998).
- [26] V. Roudnev and S. Yakovlev, Investigation of $^4\text{He}_3$ trimer on the base of Faddeev equations in configuration space, *Chem. Phys. Lett.* **328**, 97 (2000).
- [27] A. K. Motovilov, W. Sandhas, S. A. Sofianos, and E. A. Kolganova, Binding energies and scattering observables in the $^4\text{He}_3$ atomic system, *Eur. Phys. J. D* **13**, 33 (2001).
- [28] M. Salci, E. Yarevsky, S. B. Levin, and N. Elander, Finite element investigation of the ground states of the helium trimers $^4\text{He}_3$ and $^4\text{He}_2^3\text{He}$, *Int. J. Quantum Chem.*, **107**, 464 (2007).
- [29] D. Blume and Ch. H. Greene, Monte Carlo hyperspherical description of helium cluster excited states, *J. Chem. Phys.* **112**, 8053 (2000).
- [30] R. Guardiola, O. Kornilov, J. Navarro, and J. P. Toennies, Magic numbers, excitation levels, and other properties of small neutral ^4He clusters ($N \leq 50$), *J. Chem. Phys.* **124**, 084307 (2006).
- [31] R. Lazauskas and J. Carbonell, Description of ^4He tetramer bound and scattering states, *Phys. Rev. A* **73**, 062717 (2006).
- [32] E. Hiyama and M. Kamimura, Variational calculation of ^4He tetramer ground and excited states using a realistic pair potential, *Phys. Rev. A* **85**, 022502 (2012).
- [33] B. D. Esry, C. D. Lin, and C. H. Greene, Adiabatic hyperspherical study of the helium trimer, *Phys. Rev. A* **54**, 394 (1996).
- [34] T. Gonzalez-Lezana, J. Rubayo-Soneira, S. Miret-Arts, F. A. Gianturco, G. Delgado-Barrio, and P. Villarreal, Efimov States for ^4He Trimers? *Phys. Rev. Lett.* **82**, 1648 (1999).
- [35] M. Gattobigio, A. Kievsky and M. Viviani, Spectra of helium clusters with up to six atoms using soft-core potentials, *Phys. Rev. A* **84**, 052503 (2011).
- [36] L. Platter, H.-W. Hammer, and Ulf-G. Meiner, Four-boson system with short-range interactions, *Phys. Rev. A* **70**, 052101 (2004).
- [37] B. Bazak, M. Eliyahu, and U. van Kolck, Effective field theory for few-boson systems, *Phys. Rev. A* **94**, 052502 (2016).
- [38] D. M. Ceperley and M. H. Kalos, in *Monte Carlo Methods in Statistical Physics*, edited by K. Binder, (Springer, Berlin, 1979.)
- [39] M. H. Kalos, Energy of a Boson Fluid with Lennard-Jones Potentials, *Phys. Rev. A* **2**, 250 (1970).
- [40] To extract the contacts we have minimized the function $I = \int_0^{r_{90}} |\rho_n^{(N)} - C_n^{(N)} \rho_n|^2 dr$, choosing r_{90} such that $\rho_n(r_{90})$ is 90% of the n -body density peak $\rho_n(r_{peak})$, and $r_{90} \leq r_{peak}$. We have found that this procedure is robust, as replacing r_{90} by r_{85} or r_{95} affects the contacts by less than 1%.
- [41] F. H. Wirth, and R. B. Hallock, X-ray determinations of the liquid-structure factor and pair-correlation function of ^4He , *Phys. Rev. B* **35**, 89 (1987).
- [42] H. N. Robkoff, and R. B. Hallock, Structure-factor measurements in ^4He as a function of density, *Phys. Rev. B* **25**, 1572 (1982).
- [43] E. C. Svensson, V. F. Sears, A. D. B. Woods, and P. Martel, Neutron-diffraction study of the static structure factor and pair correlations in liquid ^4He , *Phys. Rev. B* **21**, 3638 (1980).
- [44] R. J. Donnelly and C. F. Barenghi, The Observed Properties of Liquid Helium at the Saturated Vapor Pressure, *J. Phys. Chem. Ref. Data* **27**, 1217 (1998).
- [45] T. R. Prisk, M. S. Bryan, P. E. Sokol, G. E. Granroth, S. Moroni, and M. Boninsegni, The Momentum Distribution of Liquid ^4He , *J. Low Temp. Phys.* **189**, 158 (2017).

Supplemental Material: Universal short range correlations in bosonic Helium clusters

The variational parameters

In Table S1 we present the trial wave function parameters (Eq. (18)) optimized with VMC calculation for small ${}^4\text{He}$ clusters $N \leq 50$.

Table S1: The optimal parameters for the trial wave function (Eq. 18).

N	p_0	p_1	p_2	p_5
2	1.	0.0309	0.3002	0.9022
3	0.5	0.2136	0.1784	0.8884
4	0.3333	0.2547	0.1774	0.8898
5	0.25	0.2654	0.2975	0.877
6	0.2	0.2279	0.1076	0.8825
7	0.1667	0.2257	0.1166	0.8844
8	0.1429	0.2063	0.1559	0.8822
9	0.125	0.1972	0.1455	0.8829
10	0.1111	0.1744	0.1202	0.8839
15	0.0714	0.1379	0.1896	0.8823
20	0.0714	0.1046	0.2401	0.881
25	0.0417	0.093	0.2526	0.8795
30	0.0345	0.0796	0.2733	0.8789
35	0.0294	0.07	0.2727	0.8801
40	0.1029	0.0405	0.3052	0.884
45	0.0926	0.0364	0.3276	0.8808
50	0.1068	0.0262	0.3326	0.8798

The contacts

In Table S2 we present the contacts for small ${}^4\text{He}$ clusters $N \leq 50$ calculated using a mixed VMC-DMC estimate. The table includes contacts $C_n^{(N)}$ for $n = 2 - 5$ coalescing particles. As explained in the main body of this manuscript, the contacts were extracted from the calculated n -particle densities $\rho_n^{(N)}(r)$.

Table S2: The numerical values of the n -body contacts in the N -body system $C_n^{(N)}$ for ${}^4\text{He}$ clusters in the range $N \in (2, 50)$, calculated using the VMC-DMC mixed estimate.

N	$C_2^{(N)}$	$C_3^{(N)}$	$C_4^{(N)}$	$C_5^{(N)}$
2	$1.00e + 00 \pm 0e + 00$			
3	$1.78e + 01 \pm 3e - 02$	$1.00e + 00 \pm 0e + 00$		
4	$4.88e + 01 \pm 1e - 01$	$6.55e + 00 \pm 4e - 03$	$1.00e + 00 \pm 0e + 00$	
5	$9.11e + 01 \pm 3e - 01$	$1.95e + 01 \pm 4e - 02$	$6.19e + 00 \pm 6e - 03$	$1.00e + 00 \pm 0e + 00$
6	$1.43e + 02 \pm 6e - 01$	$4.08e + 01 \pm 9e - 02$	$1.93e + 01 \pm 8e - 03$	$6.18e + 00 \pm 1e - 02$
7	$2.01e + 02 \pm 8e - 01$	$7.15e + 01 \pm 2e - 01$	$4.45e + 01 \pm 1e - 02$	$2.11e + 01 \pm 4e - 02$
8	$2.67e + 02 \pm 1e + 00$	$1.11e + 02 \pm 3e - 01$	$8.31e + 01 \pm 8e - 02$	$5.06e + 01 \pm 2e - 01$
9	$3.38e + 02 \pm 2e + 00$	$1.59e + 02 \pm 6e - 01$	$1.39e + 02 \pm 9e - 02$	$1.03e + 02 \pm 5e - 01$
10	$4.15e + 02 \pm 2e + 00$	$2.13e + 02 \pm 7e - 01$	$2.07e + 02 \pm 5e - 01$	$1.74e + 02 \pm 1e + 00$
15	$8.54e + 02 \pm 6e + 00$	$6.01e + 02 \pm 3e + 00$	$8.39e + 02 \pm 2e + 00$	$1.08e + 03 \pm 1e + 01$
20	$1.36e + 03 \pm 1e + 01$	$1.14e + 03 \pm 8e + 00$	$1.92e + 03 \pm 3e + 00$	$3.07e + 03 \pm 3e + 01$
25	$1.93e + 03 \pm 2e + 01$	$1.78e + 03 \pm 1e + 01$	$3.37e + 03 \pm 6e + 00$	$6.13e + 03 \pm 6e + 01$
30	$2.52e + 03 \pm 2e + 01$	$2.51e + 03 \pm 2e + 01$	$5.14e + 03 \pm 9e + 00$	$1.02e + 04 \pm 1e + 02$
35	$3.15e + 03 \pm 3e + 01$	$3.34e + 03 \pm 3e + 01$	$7.30e + 03 \pm 9e + 00$	$1.56e + 04 \pm 2e + 02$
40	$3.83e + 03 \pm 4e + 01$	$4.26e + 03 \pm 4e + 01$	$9.83e + 03 \pm 6e + 00$	$2.23e + 04 \pm 2e + 02$
45	$4.48e + 03 \pm 5e + 01$	$5.14e + 03 \pm 5e + 01$	$1.23e + 04 \pm 1e + 01$	$2.87e + 04 \pm 3e + 02$
50	$5.16e + 03 \pm 6e + 01$	$6.09e + 03 \pm 6e + 01$	$1.50e + 04 \pm 1e + 01$	$3.62e + 04 \pm 4e + 02$